1

2

3

4

5

6   **Adaptation of Saffold Virus-2 for High-Titer Growth in Mammalian Cells**

7

8   Shannon Hertzler[1], Zhiguo Liang[1], Treso Balint[1,+] and Howard L. Lipton[1,2,*]

9

10   Departments of Neurology[1] and Microbiology & Immunology[2]

11   University of Illinois at Chicago

12   835 South Wolcott Avenue

13   Chicago, Illinois 60612-7344

14

15   Abstract: 242 words

16   Text: 4198

17

18

19   [+]Present address: National Center for Epidemiology, Division of Virology, H-1097

20   Budapest, Gyali ut 2-6

21   [*]Corresponding author

22

Abstract

23

24   Saffold viruses (SAFV) are a recently discovered group of human *Cardioviruses*

25 closely related to the Theiler's murine encephalomyelitis viruses (TMEV). Unlike TMEV

26 and Encephalomyocarditis virus, each of which is monotypic, SAFV are genetically

27 diverse and include at least eight genotypes. To date, only SAFV-3 has been grown

28 efficiently in mammalian cells *in vitro*. Here, we report the successful adaptation of

29 SAFV-2 for efficient growth in HeLa cells after 13 passages in the interferon α/β-

30 deficient human glial cell line U118 MG. Nine amino acid changes were found in the

31 adapted virus, with single mutations in VP2, VP3, and 2B, while 6 mutations arose in

32 VP1. Most capsid mutations were in surface loops.   Analysis of SAFV-2 revealed virus

33 growth and cytopathic effect only in human cell lines, with large plaques forming in

34 HeLa cells, with minimal cell association, and without using sialic acid to enter cells.

35 Despite the limited growth of SAFV-2 in rodent cells *in vitro*, BALB/c mice inoculated

36 with SAFV -2 showed antibody titers $>1:10^6$, and FACS analysis revealed only minimal

37 cross-reactivity with SFV-3. Intracerebral inoculation of 6-week-old FVB/n mice

38 produced paralysis and acute neuropathological changes including meningeal infiltrates,

39 encephalitis, particularly of the limbic system, and spinal cord white matter

40 inflammation.

41   Newly identified human *Cardioviruses* (13), variously referred to as Saffold viruses

42   (SAFV), human Theiler's-like cardioviruses and Saffold-like cardioviruses, are closely

43   related to Theiler's murine encephalomyelitis viruses (TMEV) isolated more than 75

44   years ago from colony-bred mice with spontaneous paralysis (27). Phylogenetic

45   analysis has placed these viruses in the Theilovirus species of the *Cardiovirus* genus in

46   the family *Picornaviridae,* along with mouse and rat TMEV and, putatively, Vilyuisk

47   encephalomyelitis virus. The *Cardiovirus* genus also contains another species,

48   encephalomyocarditis virus (EMCV), which has a broad host range and also infects

49   humans (18, 26). Recently, Drexler et al. (6) argued that TMEV and the human

50   *Cardioviruses* represent distinct species. To date an official taxonomic name for the

51   SAFV remains to be assigned.

52

53   The initial report of a SAFV described the amplification of the virus after mouse

54   brain passage of stock isolated from the feces of an 8-month-old infant with fever of

55   undetermined origin (13). That report has now been followed by numerous clinical and

56   epidemiological publications (1, 3-7, 12, 22, 29), presaging the prevalence of these

57   emerging viruses in the human population. Most have reported the molecular detection

58   of SAFV from respiratory swab and fecal samples of young children with upper

59   respiratory and gastrointestinal illnesses, respectively. Since viruses detected in the

60   gastrointestinal and respiratory tracts may be harmless (commensals), evidence that a

61   particular virus causes the illness is based on a 4-fold or greater rise in anti-viral

62   antibody titer in convalescent serum. However, some SAFV genotypes are difficult to

63   propagate (see below), complicating the demonstration of seroconversion linking SAFV

3

64   to illnesses (4). For example, a recent study of households with gastroenteritis in which

65   a 16-month-old infant with a diarrheal illness seroconverted for SAFV-2 but not two

66   adults who did not become ill (4). Chiu et al. (4) found no cytopathic effect (cpe) of

67   SAFV-2 in LLMCK2 cells and were only able to determine antibody titers in neutralized

68   compared to control virus lysates by measuring viral RNA copies using real-time RT-

69   PCR.

70

71   Unlike TMEV and EMCV, which are monotypic, SAFV are genetically diverse and

72   include at least eight genotypes (3). The genotype classification was based on that

73   used for the *Enterovirus* genus where viruses with <87.5% VP1 amino acid similarity are

74   assigned to separate genotypes (19). Experience has shown that for the *Enteroviruses*,

75   genotype corresponds to serotype (19). The SAFV-1, -2 and -3 genotypes are globally

76   distributed and circulating in North and South America, Europe and China (1, 3-5, 7, 12,

77   22, 23, 29), while SAFV-4 to -8 have been found only in South Asia (3). Since VP1

78   surface amino acids are involved in receptor binding, this high degree of SAFV genetic

79   diversity raises the possibility that different SAFV genotypes use different protein entry

80   receptors and possess tropism for different organ systems. On the other hand, different

81   Enterovirus serotypes can also use the same receptor. To date, the identity of SAFV

82   receptors is unknown and the spectrum of disease(s) caused by SAFV remains unclear.

83

84   Only SAFV-3 has been successfully grown in mammalian cells (29). SAFV-1,

85   isolated in 1981, was originally grown in human fetal diploid kidney (HFDL) cells and

86   suckling mice; however, infection of mammalian cells, including HFDL, with virus stocks

4

87   thawed after frozen storage for more than 25 years produced no cpe, although SAFV-1

88   was detectable by RT-PCR (David Schnurr, personal communication). SAFV-2 was

89   reported to produce either minimal, nonprogressive cpe (1) or no cpe at all (4) in

90   LLCMK2 rhesus monkey kidney cells.

91

92   In the present study, we adapted SAFV-2 to grow to ~10^8 $TCID_{50}$/ml in HeLa cells

93   within 24 h, with the adapted virus acquiring 9 mutations, 6 of which were on surface

94   loops in the capsid. Growth properties of SAFV-2 were evaluated with respect to

95   plaque phenotype, single-step growth kinetics, sensitivity to neuramindase, cell

96   association, and virion morphology. Mice inoculated intracerebrally with the adapted

97   SAFV-2 were examined for SAFV-2 antibody and neuropathology.

98 **Materials and Methods**

99 **Viruses and cells.** SAFV-2 was provided by Guy Bovin at the Centre de

100 Recherche en Infectiologie, Ste-Foy Quebec, Canada (1) and SAFV-3 by F. J. M. van

101 Keppeveld at the University of Nijmegan, The Netherlands. The origin and passage

102 history of high-neurovirulence GDVII and low-neurovirulence BeAn Theiler's virus

103 stocks has been described (24). BHK-21 cells (ATCC CCL-10) were grown in

104 Dulbecco's minimum essential medium (DMEM) containing 2 mM L-glutamine, 100

105 mg/ml streptomycin, 100 U/ml penicillin, 7.5% tryptose phosphate and 10% fetal bovine

106 serum (FBS). GDVII and BeAn virus plaque formation was assayed in BHK-21 cells as

107 described (24). LLCMK2 monkey kidney cells [American Type Culture Collection

108 Manassas, VA, (ATCC) CCL-7] and grown in minimal essential medium (MEM;

109 InVitrogen-Life Technologies, Carlsbad, CA) containing 25 mM HEPES and 10% FBS at

110 37°C in a 5% CO_2 atmosphere. U118 MG human malignant glial cells (ATCC HTB-15)

111 were grown in DMEM supplemented with 10% FBS at 37°C in a 5% CO_2 atmosphere.

112 HeLa cells (ATCC CCL-2) were grown in MEM supplemented with 1% non-essential

113 amino acids and 10% FBS at 37°C in a 5% CO_2 atmosphere. Mouse sarcoma 180

114 cells (ATCC TIB-66) were grown in DMEM containing sodium pyruvate and 10% FBS at

115 37°C in a 5% CO_2 atmosphere. 293T, HepG2 (ATCC HB-8065) and Huh7 cells (JCRB

116 cell bank) were grown in RPMI supplemented with 1% non-essential amino acids, 10

117 mM HEPES (pH 7.5) and 10% FBS at 37°C in a 5% CO_2 atmosphere. Caco-2 (ATCC

118 HTB-37), T84 (ATCC CCL-248) and HT29 colon cells (ATCC HTB-38) were grown in

119 DMEM and 10% FBS at 37°C in a 5% CO_2 atmosphere.

120

121   **Virus infections.** SAFV-2 infections, $TCID_{50}$, and plaque formation was assayed

122   on 90% confluent HeLa cell monolayers in MEM medium containing 1% non-essential

123   amino acids and 1% FBS. Plaque sizes were determined based on crystal violet

124   staining of HeLa monolayers in 35-mm multi-well plates at 3 days post-infection (p.i.).

125     $TCID_{50}$ assays were performed on HeLa cell monolayers in 96-well microtiter dishes

126   based on crystal violet staining at 4 days p.i.

127

128   **Mice, inoculations and histology.** All mice were housed in the UIC Biological

129   Resource Laboratory in accordance with the standards of the UIC Animal Care

130   Committee and the NIH Guide for the Care and Use of Laboratory Animals. Female

131   BALB/c mice, 6 to 8 weeks-old, (Charles River Laboratories, Wilmington, MA), were

132   inoculated 4 times subcutaneously (s.c.) with 25-50 μg of purified SAFV-2 in an equal

133   volume of complete or incomplete Freund's adjuvant, followed by intraperitoneal (i.p.)

134   injection of 1×10^{7} Sarcoma 180 cells. Mice were sacrificed 7-10 days later for sera

135   and ascitic fluid. Five-to 6-week-old FVB/n mice of either sex were anesthetized i.p.

136   with Ketamine (31 mg/ml; Abbott, North Chicago, IL): Xyalazine (6 mg/ml; Lloyd

137   Laboratories, Shenadoah, IA) (2:1 ratio), inoculated in the right cerebral hemisphere

138   (i.c.) with 0.03 ml of virus, and observed for signs of illness for 14 days. Anesthetized

139   mice were perfused with phosphate-buffered saline (PBS, pH 7.4) and 10% buffered

140   formalin for paraffin embedding of the brains and spinal cord and staining sections with

141   hematoxylin and eosin.

142

143   **Single-step virus growth kinetics.** HeLa cell monolayers were infected at a moi

7

144   of 100 in 12-well dishes. Following adsorption for 45 min at room temperature,

145   monolayers were washed twice with MEM and incubated in MEM maintenance medium.

146   At each time point, triplicate wells were harvested and stored at -80°C. Virus lysates

147   were then frozen and thawed 3 times and cellular debris removed by low-speed

148   centrifugation. Virus titers were determined by standard $TCID_{50}$ analysis on HeLa cell

149   monolayers in 96-well microtiter plates. Results are given as the mean $\pm$ SEM of

150   triplicate samples (3 independent experiments).

151

152   **Virus binding assay.** Binding was assayed by attachment of [^{35}S]methionine-

153   labeled virus to BHK-21 or HeLa cells. Cells were detached from monolayers with Ca^{++}

154   and Mg^{++}-free PBS, washed, and resuspended to a concentration of 4×10^6 cells/ml in

155   DMEM containing 20 mM HEPES and 1% BSA for BeAn virus and SAFV-2 binding, and

156   1×10^6 cells/ml for GDVII binding, and incubated on ice for 1 h before addition of labeled

157   virus (500 particles/cell for BeAn and SAFV-2 and 20,000 particles/cell for GDVII). Cells

158   were treated with either 1 mU/ml of *Clostridium perfringens* neuraminidase for 45 min at

159   37°C or with buffer alone. Cell-associated radioactivity was measured with a

160   scintillation counter as described (11).

161

162   **Virus purification.** HeLa cell monolayers in 150-mm dishes were washed twice

163   with MEM and infected with SAFV-2 at a moi of ~10. After incubation for 45 min at

164   room temperature, MEM maintenance medium was added to the plates and incubation

165   continued at 37°C until complete cpe was observed 24 h p.i. HEPES (to a final

166   concentration of 25 mM) and $MgCl_2$ (to a final concentration of 20 mM) were added to

167   cells and supernatant followed by addition of bovine pancreatic DNase I (Sigma

168   Chemical) to a concentration of 10 μg/ml. The lysate was incubated for 30 min at room

169   temperature, brought to 1% NP-40 and stirred for an additional 30 min at room

170   temperature. After addition of 0.5 M NaCl and 10% PEG-8000 (wt/vol), the lysate was

171   stirred overnight at 4°C and centrifuged in a Beckman HB-6 rotor at 10,000 × g for 30

172   min at 4°C. The pellet was suspended in ~10% of the original volume in low-salt TNE

173   buffer (20 mM Tris-HCl, pH 7.6, 0.1 M NaCl, 2 mM EDTA) and layered over a 0.5 ml

174   30% sucrose cushion in high-salt TNE containing 1% BSA, and centrifuged in a

175   Beckman SW 50.1 rotor at 45,000 rpm for 90 min at 10°C. The pellet was suspended in

176   2 ml of low-salt TNE containing 1% BSA and 0.1% 2-mercaptoethanol, was layered onto

177   a 20 - 70% sucrose gradient in high-salt TNE and centrifuged in a SW41 rotor at 35,000

178   rpm for 3 h at 4°C.   Gradients were fractionated from the top into 0.5-ml aliquots, and

179   the virus-containing fractions (~1/3 from the bottom of the gradient) were identified by

180   OD 260/280 nm measurements of each gradient fraction. The number of virus particles

181   was determined from the virus RNA content measured at OD 260 nm. Virus-containing

182   fractions were combined, diluted in high-salt TNE to 5X the original volume, pelleted by

183   centrifugation at 45,000 rpm in a Beckman SW 50.1 rotor for 90 min at 4°C and

184   resuspended in TNE.

185

186   **ELISA.** Wells of polystyrene microtiter plates (Corning Costar, Corning, NY) were

187   coated overnight at 4°C with 50 μl of purified SAFV-2 (2 μg/ml) in PBS, washed twice

188   with PBS, blocked for 1 h at room temperature with 200 μl of 3% (wt/vol) BSA-PBS and

189   washed twice with PBS before addition of 50 μl of serially diluted serum to each well

190   and incubation for 1 h at 37°C. Unbound antibody was removed by washing twice with

191   PBS, before addition of 50 μl of goat anti-mouse IgG peroxidase diluted 1:500 in 3%

192   BSA-PBS and development with 3,3',5,5', tetramethylbenzidine. Titers were measured

193   by standard ELISA at 450-nm.

194

195   **Real-time RT-PCR.** Real-time RT-PCR (Applied Biosystems, Shelton, CT), was

196   used to quantitate SAFV-2 RNA copy numbers as described for TMEV (28). Reverse

197   transcription reactions were primed with random hexamers (InVitrogen), amplified with

198   forward primer 5' CTGGCTAATCAGAGGAAAGTCAG 3' (nucleotides 189-211) and

199   reverse primer 5' AAGATGTTAATTCCAACCACGTC 3', and detected with 5' 6FAM-

200   CGGAACGAGAAGTTCTCCCTCCC-TAMRA (nucleotides 276-298; Integrated DNA

201   Technologies, Coraville, IA).

202

203   **Microscopy.** M1-D cells were harvested and fixed with 3% glutaraldehyde in PBS.

204   Cell were further fixed in aqueous 2% osmium tetroxide, stained with 0.5% aqueous

205   uranyl acetate, dehydrated with a graded ethanol series and embedded in Epoxy Resin

206   LX112. Transverse sections (1-μm) were cut and further stained with toluidine blue O

207   for light microscopy. For transmission electron microscopy, sections were cut at 100-

208   nm thickness, placed on Formvar-coated 200 mesh copper grids, stained further with

209   uranyl acetate and lead citrate, and viewed under a JEOL model 1220 (Tokyo, Japan)

210   at 80 kV and with 1000-150,000X magnification. Images were documented with a

211   Gatan multiscan camera model 794.

212

10

213   **Molecular graphics of capsid mutations.** SAFV-2 adaptation mutations on the

214   surface of a Cα–carbon pentamer model were generated using PyMol (PyMol Molecular

215   Graphics System, version 1.4, Schrodinger, LLC) and the BeAn virus pdb1tme

216   coordinates.

217

218   **Statistical analysis.** Paired Student's t-test was used to compare groups, and

219   differences were considered significant at $p < 0.05$.

220   **Results**

221   **Adaptation of SAFV-2 in HeLa cells.** A stock of SAFV-2 grown in LLCMK2

222   cells was provided by Abed et al. (1) and produced limited cpe in LLCMK2 cells at 6-9

223   days p.i. on the initial passage. In abnormal areas, small clusters of rounded cells

224   slightly above the plane of an incomplete monolayer were observed, with dividing cells

225   subsequently filling in empty spaces in the monolayer (Fig. 1A,B). Progeny virus was

226   passed another 7 times in LLCMK2 cells, and although real-time RT-PCR revealed a 2-

227   3 log increase in viral RNA copy numbers over 10 days p.i. during these passages (Fig.

228   1C), cpe did not increase appreciably. Because the innate immune response may have

229   inhibited virus growth and thus the chance of mutations that enable adaptation, the IFN-

230   defective human glioblastoma cell line U118 MG (20) was infected with the P8 LLCMK2

231   clarified cell lysate. Considerable cpe was observed after 3-4 passages in U118 MG

232   cells but only after 7 days p.i. (Fig. 1E,F). By passage 7, extensive cpe developed

233   within 3 days (2 x 10^6 $TCID_{50}$/ml) and at passage 13, complete cpe developed within 24

234   h (5 x 10^6 $TCID_{50}$ /ml). The P13 U118 MG cell-adapted virus produced complete cpe

235   within 24 h in HeLa cells after several passages, yielding 10^7 $TCID_{50}$ /ml (Fig. 1 G,H),

236   and was used in subsequent studies without plaque purification. Fig. 1D shows the

237   passage scheme in the different cell lines.

238

239   **Amino acid changes in HeLa cell-adapted SAFV-2.** The complete genomes of

240   the initial passage of SAFV-2 in LLCMK2 cells and the HeLa cell-adapted virus were

241   sequenced. There were 22 differences in the nucleotide sequence encoding the

242   polyprotein (P1 - 15; P2 - 4; P3 - 3) between the fully adapted SAFV-2 and the

12

243   sequence of the parental virus isolated in LLCMK2 cells children with upper respiratory

244   infections (accession number AM92293).   The noncoding ends of the parental SAFV-1

245   were not sequenced. Of 9 amino acid changes in the adapted virus, single mutations

246   were present in VP2, VP3, and 2B, and 6 mutations in VP1.   Based on the relatedness

247   of SAFV and TMEV and the available 2D structures for the TMEV capsid proteins (9,

248   14, 15), 5 of 7 substitutions and a deletion were present in the sets of prominent surface

249   loops in VP2 and VP1. These changes included L2174F in the VP2 EF sequence (puff

250   B), D1080G in the VP1 CD sequence (loop I), and D1097deletion, T1098A, Q1100R,

251   and T1101I in the VP1 CD sequence (loop II) (Fig. 2A). By convention the first digit

252   designates the viral protein, in this case a capsid protein, and the following three digits

253   indicate the amino acid position in the protein. The two other amino acid substitutions in

254   the capsid were L3084P in the VP3 first corner and S1262Y in the VP1 C-terminus, the

255   highest elevation on the capsid and in contact with the VP3 knob. Figure 2B shows the

256   clustering of these mutations in the VP1 loops in a Cα-carbon pentamer model

257   generated using PyMol and the BeAn virus pdb1tme coordinates. A single mutation

258   L55P in protein 2B in the nonstructural proteins was also present. The capsid mutations

259   and single deletion that arose during adaptation might represent changes influencing

260   the interaction of SAFV-2 with its receptor.

261

262   **Host range of HeLa cell-adapted SAFV-2 in mammalian cells.** Eight human

263   (HeLa, U118 MG, Caco, T84, HT29, Hep2G, Huh7 and 293T), two non-human primate

264   (LLCMK2, BSC-1) and two rodent (BHK-21 and L929) cell lines grown in 96-well

265   mictotiter plates were inoculated with serial 10-fold dilutions of virus and the $TCID_{50}$

13

266   endpoint was determined by visual assessment of cpe and crystal violet staining of

267   monolayers (not shown). Of the human cell lines, only HeLa ($TCID_{50} = 10^{7.78}$) and U118

268   MG ($TCID_{50} = 10^{7.77}$) cells used for adaptation were susceptible to infection; three

269   intestinal cell lines (CaCo, T84 and HT29) were not susceptible to SAFV-2, despite the

270   implication of this virus in gastroenteritis. Only limited susceptibility of the non-human

271   primate cell lines ($TCID_{50} < 1.0$) was observed, while the rodent cell lines were resistant

272   to infection.

273

274   **SAFV-2 growth kinetics.** At high multiplicity of infection (moi = 100), SAFV-2

275   grown in HeLa cells showed typical single-step growth kinetics resembling that of other

276   picornaviruses, reaching high virus yields at 14 h p.i. with virus titers increased slightly

277   by 30 h p.i. (Fig. 3A). Titration indicated virus production in $TCID_{50}$/cell of 227 at 12 h

278   p.i. and 284 at 24 h. Real-time RT-PCR analysis of viral RNA replication revealed a

279   temporal profile of replication kinetics similar to that of the viral growth curve; we

280   assumed that approximately 5×10^5 viral plus strand copies were synthesized per cell

281   by 8-14 p.i. because of the predominace of plus (vs. minus strands) during picornaviral

282   RNA replication (Fig. 3B).

283

284   **SAFV- 2 relatedness to TMEV neurovirulence groups.** Unlike high-

285   neurovirulence TMEV such as GDVII, low-neurovirulence strains such as BeAn form

286   small plaques, in part because they are highly cell-associated and use sialic acid (α1-3

287   linked moieties), the most abundant negative charge on the cell-surface, as co-receptor

288   (25). Comparison of plaque formation by adapted SAFV-2 with that of high-

14

289   neurovirulence TMEV showed that SAFV-2 which was not plaque-purified, primarily

290   produced 5- to 6-mm plaques in HeLa cells after 4 days compared to 5- to 6-mm

291   plaques formed by GDVII virus and 1-mm plaques by BeAn virus in BHK-21 cells for 3

292   and 4 days, respectively (Fig. 4A-C). SAFV-2 was only partially cell-associated

293   compared to BeAn virus (Fig. 4D), and unlike BeAn bound to the same extent after

294   incubation of the cells with neuraminidase for 60 min at 37°C as with buffer alone (Fig.

295   4E).

296

297   Electron microscopic analysis of SAFV-2-infected HeLa cells revealed typical

298   cytoplasmic vesicles, which are rearrangements of cellular membranes (viroplasm), and

299   clusters of small numbers of 27-nm virions interspersed throughout the viroplasm at 10-

300   12 h p.i. (Fig. 5). This profile differs from that of TMEV, which instead display either

301   large paracrystalline arrays of virions in the case of high-neurovirulence strains or

302   mature virions aligned single-file between two unit membranes in and outside of cells

303   late in the infection with low-neurovirulence strains (8).

304

305   **Generation of high-titered antibodies and development of encephalomyelitis**

306   **in SAFV-2 infected mice.** Because SAFV-2 did not grow in L929 and BHK-21 cells, no

307   induction of CNS disease was expected in mice injected with SAFV-2. BALB/c mice

308   immunized with purified SAFV-2 in Freund's adjuvent followed by ip injection of 1 x 10^{7}

309   Sarcoma 180 cells produced ascitic fluid with SAFV-2 IgG ELISA titers of >1:10^{6}. FACS

310   analysis of the ascitic fluid incubated with HeLa cells infected with SAFV-2 or -3 and

311   fixed with methanol-acetone revealed some cross-reactivity for the two viruses,

15

312   indicating that the ELISA using disrupted virions was able to distinguish between the

313   two genotypes (Fig. 6). Sera had similar high titered antibodies (not shown).

314

315   Limb paralysis was observed in FVB/n mice following i.c. inoculation of SAFV-2

316   (data not shown). The $TCID_{50}$ was determined by RT-PCR analysis of high viral RNA

317   loads in brain tissue from the same mouse strain inoculated i.c. with 10-fold dilutions of

318   SAFV-2 (5 mice per dilution), and sacrificed on day 6, i.e., the approximate time of peak

319   acute TMEV growth in brain. Using the Reed and Muench method (21), the $TCID_{50}$ was

320   calculated as $10^{5.23}$/0.03 ml. Five to 6 week-old FVB/n mice of either sex were then

321   inoculated i.c. with two doses of virus, 10^6 and 2×10^7 pfu, and monitored for

322   development of encephalitis and for CNS histopathology. One of 3 mice inoculated at

323   the lower dose and 4 of 4 mice at the higher dose developed ruffled fur, hunched

324   posture and hind-limb weakness at 3 to 6 days p.i. when the mice were sacrificed for

325   histopathology. Neuropathological changes were the same for all the diseased mice

326   (clinically unaffected mice not examined) and included microglial proliferation and

327   perivascular cuffs in the dentate gyrus of the hippocampus with complete loss of

328   dentate neurons (Fig. 7A), lymphocytic meningeal infiltrates and microglial proliferation

329   in the cerebellar molecular layer without involvement of Purkinje cells (Fig. 7B), and mild

330   meningitis and lymphocytic infiltration in the anterior white matter of the spinal cord (Fig.

331   8C). Thus, SAFV-2 at high doses causes encephalomyelitis.

16

Discussion

332

333   Small round viruses that cause gastroenteritis, e.g., astroviruses, caliciviruses, and

334   picornaviruses, are often not grown readily or at all in cell culture. SAFV-2 is also

335   difficult to grow and quantities have not been available to sufficiently partially purify virus

336   for serology, hindering studies to determine the full clinical spectrum of this virus

337   infection.

338   SAFV-2 was originally recognized by the onset of cpe in rhesus monkey kidney

339   LLCMK2 cells 6 days after inoculation with virus from a throat swab of a young child

340   hospitalized for an upper respiratory illness (1). Another independent SAFV-2 isolate,

341   designated UC6, did not produce cpe in many different cell cultures and, despite

342   multiple attempts, could not be successfully propagated in culture (4). In the present

343   study, we showed that SAFV-2 passaged serially in LLCMK2, U118 MG and HeLa cells

344   grows efficiently to high titer and progresses rapidly to complete cpe (within 24 h p.i.) in

345   HeLa cells (Fig. 1). Technically, blind passage was not necessary in LLCMK2 cells

346   since minimal cpe was observed in the initial passage; however, with continued

347   passage, cpe did not progress. By contrast, two blind passages were required before

348   cpe was observed in U118 MG cells infected with the LLCMK2 P8 virus lysate, with

349   more rapid onset of cpe upon continued passage.

350   Adaptation of SAFV-2 led to 9 mutations in the viral genome. Five of the mutations

351   were in the two prominent sets of surface loops in the capsid, i.e., the VP2 EF (puffs A

352   and B) and the VP1 CD (loops I and II) loops. Based on reasonable alignment of the

353   SAFV-2 capsid amino acid sequence and the available molecular structures of EMCV

354   and TMEV (9, 14-16), these surface loops border the pit, a 25 Å depression thought to

17

355   be the docking site for the protein entry receptor. This function of the pit is supported by

356   studies of CD155, the poliovirus receptor that binds in an analogous depression to the

357   pit, the canyon that surrounds around the 5-fold axis of the poliovirion (2, 10). Receptor

358   usage exerts a major influence on viral host range. These 5 mutations in the SAFV-2

359   capsid were probably selected for increased binding affinity and/or facilitation of virus

360   entry into HeLa cells. Two other mutations also present in the capsid (L3084P in the

361   VP3 first corner and S1262Y in the VP1 C-terminus) were more distant from the pit,

362   whereas only a single mutation was found in a nonstructural protein, L55P in protein 2B.

363   The exact role of the mutations awaits identification of the SAFV-2 receptor(s) and

364   studies of SAFV-2-receptor interactions.

365

366   The only other SAFV that has been grown efficiently in mammalian (HeLa) cells is

367   SAFV-3, which enabled a seroepidemiological study showing that infection in humans

368   occurs primarily by 2 years of age, with seroprevalence reaching 90% in 10 year-olds

369   (29). The molecular detection of SAFV-3 in young children with gastroenteritis, upper

370   respiratory illnesses and exudative tonsillitis as well as in normal individuals, also

371   supports a young age of infection (1, 5, 7, 12, 23). Thus, a small proportion of older

372   children and adults remain susceptible to this virus and may be subject to more severe

373   illness as a result of delayed infection. Recently, Chiu et al. (4) reported that 75% of

374   adults were seropositive for SAFV-2; however, unconventional serological methods

375   were used in that study and those results await confirmation by neutralization testing or

376   ELISA.

377

378   Although SAFV are global in distribution, several surveys of large numbers of

379   patients with gastroenteritis and upper respiratory illnesses detected SAFV sequences

380   in less than 1% of cases (3, 5, 7, 22, 23), and SAFV genotypes 4 to 8 have been found

381   only in South Asia (3). Those findings differ from the seasonal occurrence of human

382   enteroviruses where circulating viruses may be isolated or amplified from 5 to 10% of

383   cases. However, SAFV-4 to -8 were amplified from the feces of Southeast Asian

384   children with flaccid paralysis as well as normals (controls), and SAFV-2 has been

385   associated with a small outbreaks of gastroenteritis in families (4). Recently, SAFV-2

386   was amplified from throat swabs of 9 of 37 cases (24%) of exudative tonsillitis in young

387   children in Yagata, Japan (12), a finding that awaits confirmation.

388

389   Here we showed that high doses of SAFV-2 inoculated ic into adult mice produced

390   paralysis and neuropathological changes consistent with acute encephalomyelitis,

391   particularly in the limbic system. Mononuclear cell infiltrates were also seen in the

392   anterior white matter of the spinal cord, overlying meningitis in the same anterior

393   location as early lesions observed during persistent low-neurovirulence TMEV infection

394   in mice. Although cerebellar lesions have not been observed in TMEV-infected mice,

395   SAFV-2 infection resulted in patchy areas of microglial proliferation in the cerebellum

396   but without involvement of Purkinje cells. These observations do not assure SAFV-2

397   neurotropism since even non-encephalitic arthropod-borne viruses induce encephalitis

398   in mice. However, they suggest that SAFV-2 has neurotropic potential. Further clinical

399   information and experimental infection of primates might shed light on this question.

400

19

408 **References**

409 1. **Abed, Y., and G. Boivin.** 2008. New Saffold cardiovirus in 3 children in Canada.

410   Emerg. Infect. Dis. **14:**834-836.

411 2. **Belnap, D. M., B. M. McDermott, Jr., D. J. Filman, N. Cheng, B. L. Trus, H. J.**

412   **Zuccola, V. R. Racaniello, J. M. Hogle, and A. C. Steven.** 2000. Three-

413   dimensional structure of poliovirus receptor bound to poliovirus. Proc. Natl. Acad.

414   Sci. U. S. A. **97:**73-78.

415 3. **Blinkova, O., A. Kapoor, J. Victoria, A. Naeem, S. Shaukat, S. Sharif, M. M.**

416   **Alam, M. Angez, S. Zaidi, and E. L. Delwart.** 2009. Cardioviruses are

417   genetically diverse and common enteric infections in South Asian children. J.

418   Virol. **83:**4631-4641.

419 4. **Chiu, C. Y., A. L. Greninger, E. C. Chen, T. D. Haggerty, J. Parsonnet, E.**

420   **Delwart, J. L. DeRisi, and D. Ganem.** 2010. Cultivtion and serological

421   characterization of a human Theiler's-like cardiovirus associated with diarrheal

422   disease. J. Virol. **84:**4407-4414.

423 5. **Chiu, C. Y., A. L. Greninger, K. Kanada, T. Kwok, K. F. Fischer, C. Runckel,**

424   **J. K. Louie, C. A. Glaser, S. Yagi, D. P. Schnurr, T. D. Haggerty, J.**

425   **Parsonnet, D. Ganem, and J. L. DeRisi.** 2008. Identification of cardioviruses

426   related to Theiler's murine encephalomyeltiis virus in human infections. Proc.

427   Natl. Acad. Sci. U.S.A. **105:**14124-14129.

428 6. **Drexler, J. F., S. Baumgarte, L. K. de Souza Luna, A. Stocker, P. S. Almeida,**

429   **T. C. M. Ribeiro, N. Petersen, P. Herzog, C. Pedroso, C. Brites, H. da Costa**

430   **Ribeiro Jr., A. Gmyl, C. Drosten, and A. Kukashev.** 2010. Genomic features

431   and evolutionary constraints in Saffold-like cardioviruses. J. Gen. Virol. **91:**1418-

432   1427.

433 7.   **Drexler, J. F., L. K. de Souza Luna, A. Stocker, P. S. Almeida, T. C. M.**

434   **Ribeiro, N. Peterson, P. Herzog, C. Pedroso, H. I. Huppertz, H. da Costa**

435   **Ribeiro Jr, S. Baumgarte, and C. Drosten.** 2008. Circulation of 3 lineages of a

436   novel Saffold cardiovirus in humans. Emerg. Infect. Dis. **14:**1398-1405.

437 8.   **Friedmann, A., and H. L. Lipton.** 1980. Replication of GDVII and DA strains of

438   Theiler's murine encephalomyelitis virus in BHK 21 cells: An electron microscopic

439   study. Virology **101:**389-398.

440 9.   **Grant, R. A., D. J. Filman, R. S. Fujinami, J. P. Icenogle, and J. M. Hogle.**

441   1992. Three-dimensional structure of Theiler's virus. Proc. Natl. Acad. Sci. U. S.

442   A. **89:**2061-2065.

443 10. **He, Y., V. D. Bowman, S. Mueller, C. M. Bator, J. Bella, X. Peng, T. S. Baker,**

444   **E. Wimmer, R. J. Kuhn, and M. G. Rossmann.** 2000. Interaction of the

445   poliovirus receptor with poliovirus. Proc. Natl. Acad. Sci. U. S. A. **97:**79-84.

446 11. **Hertzler, S., M. Luo, and H. L. Lipton.** 2000. Mutation of predicted virion pit

447   residues alters binding of Theiler's murine encephalomyelitis virus to BHK-21

448   cells. J. Virol. **74:**1994-2004.

449 12. **Itagaki, T., C. Abiko, T. Ikeda, Y. Aoki, J. Seto, K. Mizuta, T. Ahiko, H.**

450   **Tsukagoshi, M. Nagano, M. Noda, T. Mizutani, and H. Kimura.** 2010.

451   Sequence and phylogenetic analyses of Saffold cardiovirus from children with

452   exudative tonsillitis in Yamagat, Japan. Sandanavian Journal of Infectious

453   Diseases **42:**early online 1-3.

454   13.   **Jones, M. S., V. V. Lukashov, R. D. Ganac, and D. P. Schnurr.** 2007.

455   Discovery of a novel human picornavirus from a pediatric patient presenting with

456   fever of unknown origin. J. Clin. Microbiol. **45:**2144-2150.

457   14.   **Luo, M., C. He, K. S. Toth, C. X. Zhang, and H. L. Lipton.** 1992. Three-

458   dimensional structure of Theiler's murine encephalomyelitis virus (BeAn strain).

459   Proc. Natl. Acad. Sci. U. S. A. **89:**2409-2413.

460   15.   **Luo, M., K. S. Toth, L. Zhou, A. Pritchard, and H. L. Lipton.** 1996. The

461   structure of a highly virulent Theiler's murine encephalomyelitis virus (GDVII) and

462   implications for determinants of viral persistence. Virology **220:**246-250.

463   16.   **Luo, M., G. Vriend, G. Kamer, I. Minor, E. Arnold, M. G. Rossmann, U.**

464   **Boege, D. G. Scraba, G. M. Duke, and A. C. Palmenberg.** 1987. The atomic

465   structure of Mengo Virus at 3.0 è resolution. Science **235:**182-191.

466   17.   **Novak, J. E., and K. Kirkegaard.** 1991. Improved method for detecting

467   poliovirus negative strands used to demonstrate specificity of positive-strand

468   encapsidation and the ratio of positive to negative strands in infected cells. J.

469   Virol. **65:**3384-3387.

470   18.   **Oberste, M. S., E. Gotuzzo, P. Blair, W. A. Nix, T. G. Kziazek, and J. A.**

471   **Comer.** 2009. Human febrile illness caused by encephalomyocarditis virus

472   infection, peru. Emerg. Infect. Dis. **15:**640-646.

473   19.   **Oberste, S. M., K. Maher, D. R. Kilpatrick, and M. A. Pallansch.** 1999.

474   Molecular evolution of human enteroviruses: correlation of serotype with VP1

475   sequence and application to picornavirus classification. J. Virol. **73:**1941-1948.

476 20. **Ponten, J., Macintyre, E. H.** 1967. Long term culture of normal and neoplastic

477 human glia. Acta Pathol. Microbiol. Scand. **74:**465-486.

478 21. **Reed, L. J., and H. A. Muench.** 1938. A simple method of estimating fifty

479 percent endpoints. Am. J. Hygiene **27:**493-497.

480 22. **Ren, L., R. Gonzalez, Y. Xiao, X. Xu, L. Cheng, G. Vernet, G. Paranhos-**

481 **Baccala, J. Qi, and J. Wang.** 2009. Saffold cardiovirus in children with acute

482 gastroenteritis in Beijing, China. Emerg. Infect. Dis. **15:**1509-1511.

483 23. **Ren, L., R. Gonzalez, Z. Xie, Y. Li, C. Liu, L. Chen, G. Vernet, G. Paranhos-**

484 **Baccala, Q. Jin, K. Shen, and J. Wang.** 2010. Saffold cardioviruses of 3

485 lineages in children with respiratory tract infections, Beijing, China. Emerg. Infect.

486 Dis. **16:**1158-1161.

487 24. **Rozhon, E. J., J. D. Kratochvil, and H. L. Lipton.** 1983. Analysis of genetic

488 variation in Theiler's virus during persistent infection in the mouse central

489 nervous system. Virology **128:**16-32.

490 25. **Shah, A. H., and H. L. Lipton.** 2002. Low-neurovirulence Theiler's viruses use

491 sialic acid moieties on N-linked oligosaccharide structures for attachment.

492 Virology **304:**443-450.

493 26. **Tesh, R. B.** 1978. The prevalence of encephalomyocarditis virus neutralizing

494 antibodies among various human populations. Am. J. Trop. Med. Hyg. **27:**144-

495 149.

496 27. **Theiler, M.** 1934. Spontaneous encephalomyelitis of mice - a new virus disease.

497 Science **80:**122.

498 28. **Trottier, M., B. P. Schlitt, and H. L. Lipton.** 2002. Enhanced detection of

499   Theiler's virus RNA copy equivalents in the mouse central nervous system by

500   real-time RT-PCR. J. Virol. Methods **103:**89-99.

501 29. **Zoll, J., S. E. Hulshof, K. Lanke, F. V. Lunel, W. J. G. Melchers, E.**

502   **Schoondermark-van de Ven, M. Roivainen, J. Galama, and F. J. M. van**

503   **Keppeveld.** 2009. Saffold virus, a new human Theiler's-like cardiovirus, is

504   ubiquitious and causes infection early in life. PLoS Pathogens **5:**1-10.

505   **Figure Legends**

506   Fig. 1. Adapation of SAFV-2 to high-titer growth in mammalian cells. A. Mock-infected

507   LLCMK2 rhesus monkey kidney cells showing normal morphology. B. SAFV-2-infected

508   LLCMK2 cells at 8 days p.i. (LLCMK2P8) showing small clusters of rounded cells

509   slightly above the plane of the monolayer. C. Temporal analysis of SAFV RNA

510   replication in LLCMK2 cells at passage 6 by real-time RT-PCR showing a 2-log increase

511   in viral copy numbers. D. Scheme of SAFV-2 adaptation in each cell line with the

512   number of passages and development and progression of cpe over time. E. Mock-

513   infected U118 MG cells showing normal cell morphology. F. SAFV-2-infected LLCMK2

514   P8 at 3 day p.i. showing advanced cpe at passage 7.   G. Mock-infected HeLa cells

515   showing normal cell morphology. H. SAFV-2 (U118 P13)-infected HeLa cells (24 h p.i.)

516   showing advanced cpe at passage 3.

517

518   Fig. 2. A. Modified ribbon drawing of BeAn VP1, VP2 and VP3 (15), with VP1 loop I

519   shortened by four residues and VP2 puff B increased by two residues to more closely

520   resemble the SAFV-2 VP sequence. The eight capsid mutations in adapted SAFV-2

521   are indicated as a, L2174F; b, L3084P, c, D1080G; d, D1097deletion, e, T1098A; f,

522   Q1100R; g, T1101I; and h, S1262Y, where according to picornavirus convention the

523   first digit designates the capsid protein and the other three digits, the amino acid

524   number. B. SAFV-2 adaptation mutations on the surface of a Cα–carbon pentamer

525   model generated using PyMol and the BeAn virus pdb1tme coordinates. Yellow, 5

526   mutations clustered on VP1 loops I and II and one mutation in VP2 puff B; blue, VP1;

527   green, VP2; and red, VP3. VP3 mutation L3084 is not visible in this orientation of the

26

528   model and VP1 S1262Y is not evident because the VP1 C-terminal 15 residues were

529   disordered in the BeAn virus crystal structure (14).

530

531   Fig. 3. A. Single-step adapted SAFV-2 growth kinetics in HeLa cells at an moi = 100,

532   with 96% of the virus yield observed by 14 h p.i. B. SAFV-2 RNA replication kinetics.

533

534   Fig. 4. SAFV-2 plaque morphology, cell-association and sialic acid binding. A, B.

535   Plaques produced in BHK-21 cells by GDVII after 3 days and BeAn after 4 days of

536   incubation, respectively. C. SAFV-2 plaques in HeLa cells after 4 day's incubation.

537   Note that the SAFV-2 lysate was not plaque-purified and shows mainly large and some

538   small plaques. D. Cell-association determined from the ratio of the total virus yield in

539   pfu (cells and supernatant) to that in the supernatant for GDVII, BeAn and SAFV-2,

540   mean $\pm$ sd (a representative experiment of 4). E. Binding of [S^{35}]methionine-labeled

541   virions to cells in suspension after treatment with 1 mU/ml of *Clostridium perfringens*

542   neuramindase for 45 min at 37°C or with buffer alone, mean $\pm$ sd (a representative
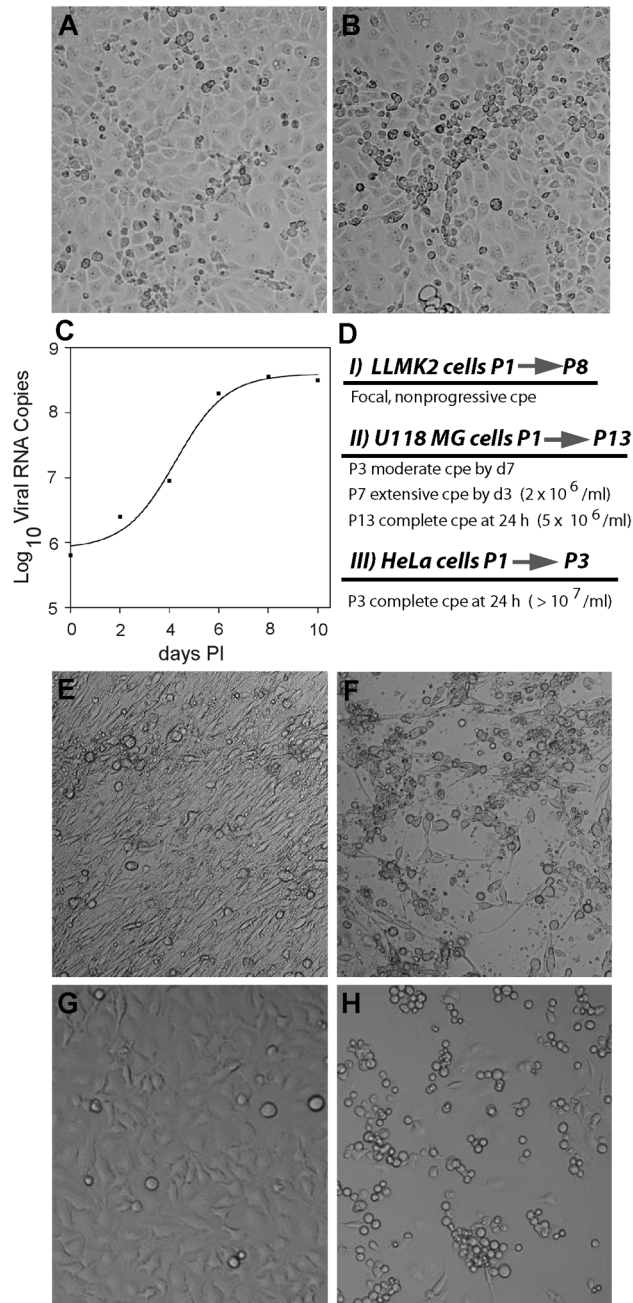
543   experiment of 3).

544

545   Fig. 5. Electron micrograph of SAFV-2-infected HeLa cells (moi = 100) for 9 h showing

546   typical picornavirus rearrangement of cellular membranes (viroplasm) with clusters of

547   more electron-dense 27-nm virions scattered throughout the viroplasm. Bar = 2 μm.

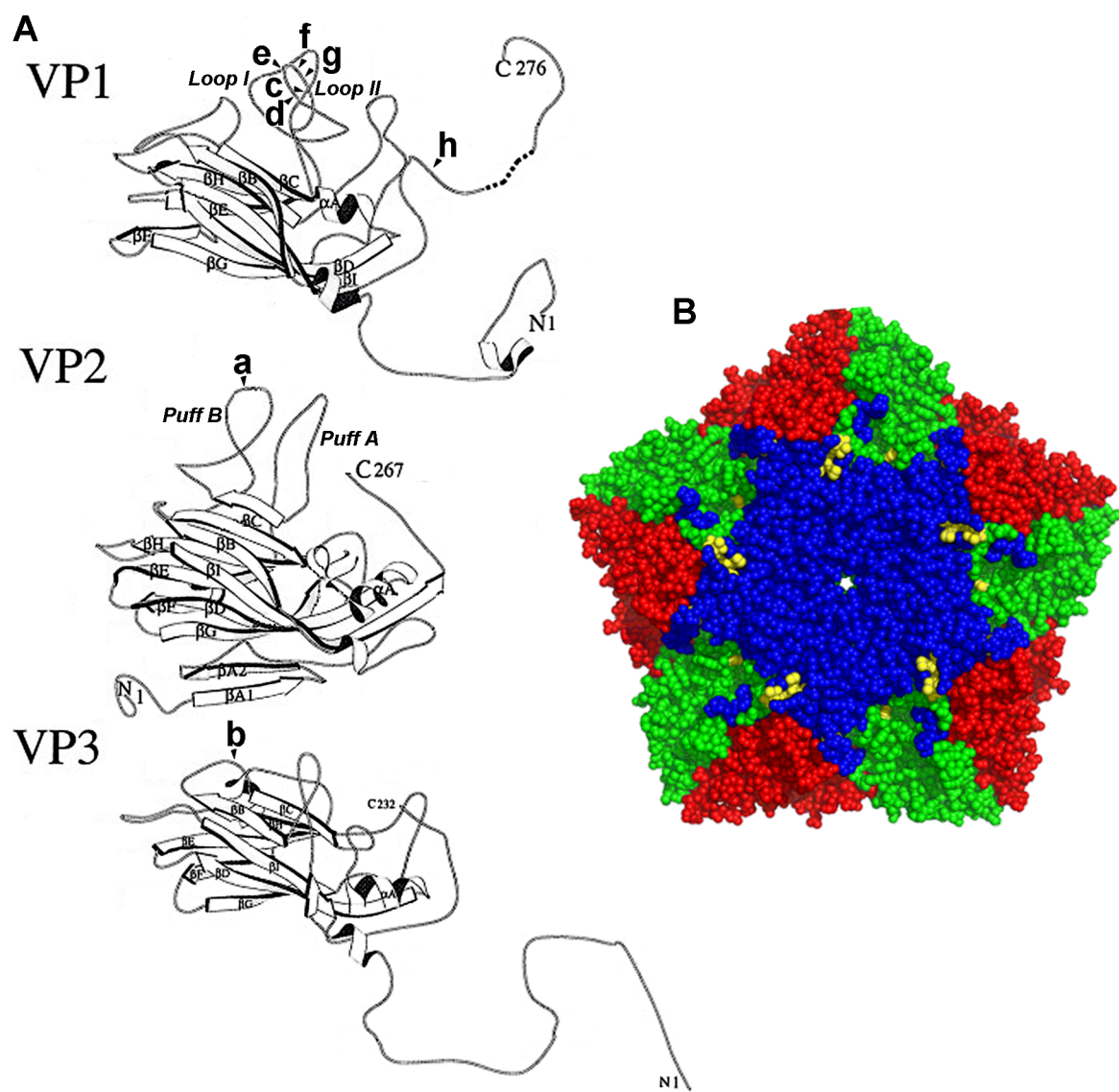548   Virions are shown at higher magnification in the insert. Bar = 0.5 μm.
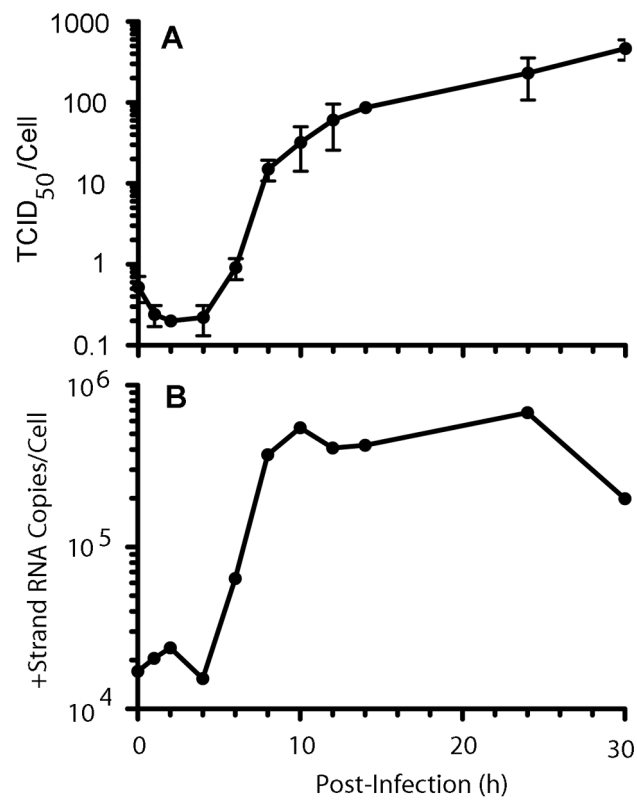
549

27

550   Fig. 6. FACS analysis of hyperimmune ascitic fluid raised in SAFV-2-injected mice and

551   incubated with SAFV-2- or SAFV-3-infected HeLa cells. HeLa cells infected at a moi =

552   5 were harvested at 16 h pi and stained with the a 1:500 dilution of hyperimmune ascitic

553   fluid and 1:50 dilution of FITC-conjugated goat anti-mouse IgG. The small peaks of

554   SAFV-2 and SAFV-3 overlapping the uninfected cell profile were probably cells that

555   were not infected.

556

557   Fig. 7. Neuropathological changes in an adult FVB/n mouse on day 6 pi after ic

558   inoculation of 1 x 10^6 pfu of SAFV. A. Microglial proliferation and perivascular cuffs in

559   the dentate gyrus of the hippocampus with loss of dentate neurons. B. Lymphocytic

560   meningeal infiltrates and microglial proliferation in the cerebellar molecular layer

561   (arrows) without involvement of Purkinje cells. C. Mild meningitis and lymphocytic

562   infiltration in the anterior white matter of the spinal cord (arrow), with sparing of the

563   anterior horn region. Hematoxylin and eosin staining.

A

B

C

Log$_{10}$ Viral RNA Copies

9

8

7

6

5

0 2 4 6 8 10

days PI

D

I) LLMK2 cells P1 → P8

Focal, nonprogressive cpe

II) U118 MG cells P1 → P13

P3 moderate cpe by d7

P7 extensive cpe by d3 (2 x 10^6/ml)

P13 complete cpe at 24 h (5 x 10^6/ml)

III) HeLa cells P1 → P3

P3 complete cpe at 24 h (> 10^7/ml)

E

F

G

H

A

VP1

Loop I e f g Loop II
c
d
C 276
h
βH βB βC
βE αA
βF
βG βD βI
N1

VP2

a
Puff B
Puff A
C 267
βC
βH βB
βE βI αA
βF βD
βG
N1 βA2
βA1

VP3

b
βB βC
βH βI
βE
βF βD αA
βG C 232
N1

B

Fig. 4

2 μm

0.5 μm